

# Preparation, characterization and dielectric, ac conductivity with electrochemical behavior of strontium zirconate

Rohan Das<sup>a</sup>, Kaushik Gupta<sup>a</sup>, Kuntal Jana<sup>a</sup>, Arabinda Nayak<sup>b\*</sup>, Uday Chand Ghosh<sup>a, b\*</sup>

<sup>a</sup>Department of Applied Chemistry, Ramakrishna Mission Vidyamandira, Belur Math, West Bengal 700012, India

<sup>b</sup>Department of Physics, Presidency University, 86/1 College Street, Kolkata 700073, West Bengal, India

\*Corresponding author. E-mail: ucghosh@yahoo.co.in, arabinda.physics@presiuniv.ac.in

Received: 11 November 2015, Revised: 02 December 2015 and Accepted: 22 May 2016

## ABSTRACT

Strontium-zirconium bimetal oxide ( $\text{SrZrO}_3$ ) samples at nanophase were prepared by chemical precipitation-annealation method, and characterized by powder X-ray diffraction (XRD), UV-Vis and FTIR spectroscopies and field emission scanning electron microscopy (FESEM). Grain size (nm) of the  $\text{SrZrO}_3$  samples prepared by annealing at 650°C (S650), 850°C (S850) and 1050°C (S1050), respectively, were 55-60, 45-47 and 25-32. The optical band gaps (eV) estimated are to be 4.71 and 4.83 of S850 and S1050, respectively. Both FTIR and XRD studies confirmed the formation of  $\text{SrZrO}_3$  phase. FESEM images of the S850 sample showed the presence of agglomerated nano spheres with irregular surface morphology. Temperature dependent ac-conductivity analyses of S850 sample showed semiconducting behavior with low thermal activation energy (28 meV). Hopping conduction of charge carriers had been concluded considering the relaxation processes associated with the grain and grain boundaries of the sample. Dielectric behavior of S850 sample was confirmed from considerably high dielectric constant value (~ 140) and low dielectric loss (~ 0.6) at 100 Hz. Cyclic voltammograms suggested the pseudo-capacitive behavior of as-prepared S850 and S1050 samples. Thus as-prepared  $\text{SrZrO}_3$  nanophase could be used as High-K dielectric material in various applications. Copyright © 2016 VBRI Press.

**Keywords:** Bimetal oxide; ac-conductivity; dielectric; electrochemical capacitor.

## Introduction

High temperature oxide materials particularly zirconates of alkaline earth metals ( $\text{SrZrO}_3$ ,  $\text{BaZrO}_3$ ,  $\text{La}_2\text{Zr}_2\text{O}_7$ , Y- $\text{SrZrO}_3$  etc) are currently gaining considerable importance in the field of electrical ceramics [1], refractories [2], luminescent [3] and heterogeneous catalysis [4]. The performance of these materials depends on the nature of precursor materials and compounds, perfection of crystal lattice and the size of the particles, which in turn depends on the synthesis procedure and conditions.  $\text{SrZrO}_3$  is an important non-ferroelectric perovskite oxide material exhibiting many important properties finds potential applications as High-K dielectric material in future memory devices and possibility of replacing silicon dioxide due to its high (~ 60) and almost temperature independent dielectric constant [5] and high mechanical strength. Different techniques have been adopted for the synthesis of  $\text{SrZrO}_3$  previously like solid state reaction [6], sol-gel technique [7], co-precipitation [8] and hydrothermal method [9]. Each of the methods of synthesis reported previously has had their own loopholes like in homogeneity, impurity contamination, non-uniform size distribution etc. However, co-precipitation method which is used in this study has some advantages due to its procedural simplicity; cost effectiveness, comparatively uniform particle size distribution etc. It has also been found in many ceramic materials that the high dielectric constant

is due to the presence of grain boundary and sub-grain boundary [10]. In view of this, study of charge carriers relaxation processes associated with the grain and grain boundary is important to understand the basic processes involved in the materials [11]. Though very limited investigations on the measurement of dielectric constant and ac conductivity at elevated temperatures are available [12-14], no such study on the ac-conductivity relaxation processes in  $\text{SrZrO}_3$  nanocrystals is found in the literature. Nevertheless, the electrochemical behaviour of the  $\text{SrZrO}_3$  nanomaterials as electrochemical capacitors is completely unknown till date.

Thus, this manuscript reports the results of dielectric behavior, temperature (24<sup>o</sup>-180<sup>o</sup>C) dependent ac-conductivity explained considering the relaxation processes associated with the grain and grain boundaries and electrochemical behavior of as-prepared nanophase crystalline  $\text{SrZrO}_3$  materials.

## Experimental

Strontium-zirconium bimetal oxide ( $\text{SrZrO}_3$ ) samples were synthesized via conversion to hydroxide-gel and incineration technique. Despite the high difference of solubility product values between  $\text{Sr}(\text{OH})_2$  and  $\text{Zr}(\text{OH})_4$ , both  $\text{Sr}^{2+}$  and  $\text{Zr}^{4+}$  ions could be co-precipitated from their mixture by sudden increase of solution pH  $\geq 13.0$ . The

definite weight amount (parenthesis) of  $\text{SrCO}_3$  (0.1476 g, 1mmol) (purity > 99.5%, Merck, Mumbai) and  $\text{ZrOCl}_2$  (0.3223 g, 1mmol) (purity > 99.5%, M/S Loba Chemicals Pvt. Ltd., India) were taken into a clean mortar and mixed (1:1, mole/mole) intimately, which was transferred to a 500 ml beaker with 100 ml of distilled water. The mixture was magnetically stirred with drop-wise addition (8 – 9 drops) of concentrated HCl (analytical grade, Merck, Mumbai) to dissolve  $\text{SrCO}_3$  and  $\text{ZrOCl}_2$  completely. To the clear solution, freshly prepared aqueous KOH (purity > 99.5%, Merck, India) solution (0.3 M) was added till the pH adjusted at  $\text{pH} \geq 13.0$ , where white precipitate appeared. The precipitate was then stirred magnetically for homogeneity for an hour. The white mass (precipitate) was finally filtered and washed several times with distilled water to remove the extraneous contaminants. Drying the precipitate in air, the solid mass was divided and transferred to the four separate silica crucibles. Each crucible including the solid mass was annealed separately at 450 °C, 650 °C, 850 °C and 1050 °C inside a muffle furnace for 2 hours. Each annealed mass in crucible was cooled to room temperature inside desiccators, and marked in accordance to annealed temperature as S450, S650, S850 and S1050.

Characterizations of the samples were carried out by Powder X-ray diffraction (XRD) (Bruker D8 Advanced, Germany), Fourier Transform Infrared Spectrometer (FTIR) (Perkin Elmer FTIR Spectrometer Spectrum II), UV-Vis spectrophotometer (Perkin Elmer UV-Vis spectrometer Lambda 25) and Field Emission Scanning Electron Microscopy (FESEM) (QUANTA FEG250).

XRD patterns of samples were taken using  $\text{Cu-K}\alpha$  radiation ( $\lambda = 0.154 \text{ nm}$ ) in a wide range of deflection angles  $2\theta$  ( $10^\circ \leq \theta \leq 80^\circ$ ) with a scanning rate of  $2^\circ/\text{min}$ . FTIR analysis of  $\text{SrZrO}_3$  samples were investigated in the range 450 to  $4000 \text{ cm}^{-1}$  using spec pure KBr pressed pellet (sample: KBr = 1:100). UV-Vis spectroscopy for the crystalline  $\text{SrZrO}_3$  powders was carried out using 10 mg powder samples/L water sonicating for 2 hours at wavelength ranged in 190 to 800 nm for band-gap. FESEM image of the powdered  $\text{SrZrO}_3$  (S850) sample was taken casting over copper grid for the surface morphology.

A large number of pellets (diameter: 13 mm, thickness: 1.2 mm) of  $\text{SrZrO}_3$  samples were made from fine grained powder (grain size:  $\sim 35 \text{ nm}$ ) using hydraulic press by applying 5-ton pressure. The pellets were sintered at  $850^\circ\text{C}$  in open atmosphere for dielectric and ac conductivity measurements. The frequency ( $f$ ) dependent real parts of the dielectric constants ( $\epsilon'$ ) for  $\text{SrZrO}_3$  were measured using a HIOKI 3532-50 LCR Hi Tester. The capacitance ( $C$ ), the imaginary part of impedance ( $Z''$ ), dielectric loss ( $\tan \delta$ ) and the conductance ( $G$ ) of the parallel plate capacitor made by the pressed pellet samples were directly measured in the frequency range 42 Hz–5 MHz at various temperatures ( $24^\circ\text{C}$ – $180^\circ\text{C}$ ). The parallel plate capacitor was constructed by applying conducting silver paste on both sides of the pressed pellets. The dielectric constant ( $\epsilon' = CL/\epsilon_0 A$ , where,  $\epsilon_0 = 8.856 \times 10^{-12} \text{ F/m}$ ) and ac conductivity ( $\sigma = GL/A$ ) were easily obtained from  $C$ ,  $G$  and the sample geometry ( $L$ =thickness and  $A$  = area of cross section).

Electrodes for  $\text{SrZrO}_3$  (S850 and S1050) supercapacitor were prepared using the procedure of Sen and Dey [15]. Electrochemical behavior of the samples through cyclic voltammetry (CV) measurement was investigated with AUTOLAB-30 potentiostat/galvanostat. A platinum electrode and a saturated Ag/AgCl electrode were used as counter and the reference electrodes, respectively. Cyclic Voltammograms were recorded between  $-0.6\text{V}$  and  $+0.6\text{V}$  against the reference electrode at a scan rate of  $20\text{mV/s}$ . Both galvanostatic charge-discharge cycling and electrochemical impedance studies were performed with two electrode system having identical electrodes made of same active electrode materials *i.e.* TYPE I electrochemical capacitor. Constant current density of  $(+ -) 1\text{mA cm}^{-2}$  was employed for charging/discharging the cell in the voltage range ( $+ 0.6\text{V}$  to  $- 0.6\text{V}$ ). Electrochemical impedance spectra (EIS) were taken over the frequency range 10 kHz to 10 MHz with potential amplitude of 5mV. All the electrochemical experiment (*i.e.* CV, charge-discharge, EIS) were carried out in an electrolyte containing 1M  $\text{LiClO}_4$  in acetonitrile.

## Results and discussion

**Fig. 1** shows the powder XRD patterns of  $\text{SrZrO}_3$  samples (S450, S650, S850 and S1050), which were prepared by annealing at four different temperatures ( $450^\circ\text{C}$ ,  $650^\circ\text{C}$ ,  $850^\circ\text{C}$  and  $1050^\circ\text{C}$ ) and that of pure oxides (inset of **Fig. 1**). Comparison of the patterns of the four synthetic samples with those of the pure oxides showed a sharp difference indicating the formation of some new phases within the crystallites. Taking a close view of **Fig. 1**, it has been seen that degree of crystalline phases increased with increase of the annealing temperature which might have influence improving the dielectric and electrical properties. XRD pattern revealed that the sample S450 is almost amorphous nature as no sharp peak appeared.

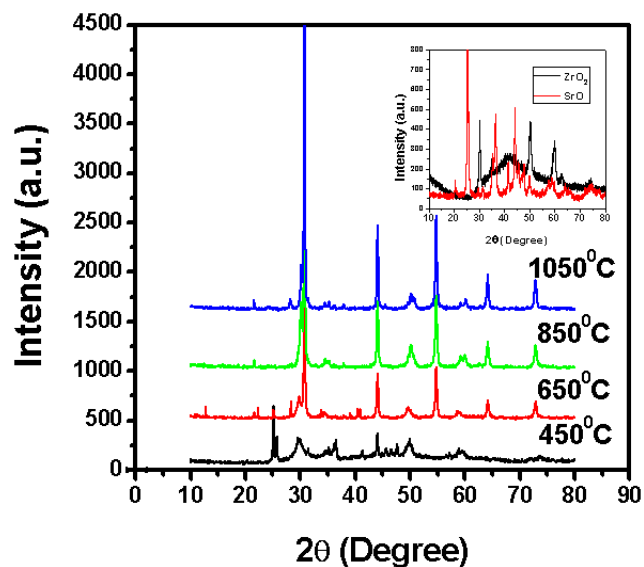


**Fig. 1.** The XRD patterns of as-prepared  $\text{SrZrO}_3$  samples including pure oxides (inset).

Three samples showed five major peaks at  $2\theta$  values of  $30.84^\circ$ ,  $44.18^\circ$ ,  $54.87^\circ$ ,  $64.26^\circ$  and  $73.00^\circ$  having ' $d_{hkl}$ '

(inter-planar distance) values of 0.29002 nm, 0.20512 nm, 0.1675 nm, 0.14497 nm and 0.12975 nm corresponding to (121), (123), (202), (161), (201) reflection planes, indicating the orthorhombic unit cell of SrZrO<sub>3</sub> with perovskite structure (JCPDS card No. 44-0161). The lattice parameters of the samples have been calculated using the following formula for orthorhombic structure.

$$\frac{1}{d_{hkl}^2} = \frac{h^2}{a^2} + \frac{k^2}{b^2} + \frac{l^2}{c^2}$$

The lattice parameters estimated for SrZrO<sub>3</sub> samples are to be as  $a = 0.5819$  nm,  $b = 0.8198$  nm,  $c = 0.5790$  nm. The presence of some unknown peaks with very low intensity indicates the samples are not 100% phase pure in nature. Some low intense peaks related to tetragonal crystal structure of SrZrO<sub>3</sub> are found to appear [16], while the characteristic diffraction peaks of SrO and ZrO<sub>2</sub> are found to disappear.

The crystallite size of the samples had been estimated using the Scherrer equation [17],

$$D = \frac{0.9\lambda}{\beta \cos\theta}$$

where,  $\lambda = 0.154$  nm,  $\beta$  is the full width at half-maximum in radians, and  $\theta$  is the angle at maximum intensity of (121) plane. Average size (nm) of the crystallites of S650, S850 and S1050 samples was ranged in 55-60, 45-47, and 25-32, respectively. The decrease of crystallite size suggested the predominance of segregation with increasing temperature of incineration. Thus, the crystallite size of SrZrO<sub>3</sub> could be tuned by annealing temperature to achieve desired property.

In A of Fig. 2 shows the FTIR spectra of two native oxides (SrO, ZrO<sub>2</sub>). The broad band appeared at a wave number  $\sim 3400$  cm<sup>-1</sup> which is due to the stretching mode of the hydroxyl group. Among the three strong bands (1475, 860 and 704 cm<sup>-1</sup>) in FTIR spectrum of SrO, the too sharp band at 1475 cm<sup>-1</sup> is due to the presence adsorbed water molecules. The bands appeared at 860 and 704 cm<sup>-1</sup> represented the Sr-O stretching and bending modes of vibration, respectively. The absorption bands at 1385, 1545 and 1628 cm<sup>-1</sup> in the FTIR spectrum of ZrO<sub>2</sub> indicated the vibration of Zr-OH bond.

In B of Fig. 2 FTIR spectra of the four as-prepared SrZrO<sub>3</sub> (S450, S650, S850 and S1050) samples. Most important information as received from the spectra is the absence of the band for surface -OH groups at wave number  $\sim 3400$  cm<sup>-1</sup>. However, the presence of a sharp band at 1475 cm<sup>-1</sup> of S450 and S650 samples indicated the existence of adsorbed water molecules but that band was absent in the FTIR spectrums of S850 and S1050, indicating complete removal of water. However, very few -OH groups are still retained on S1050 sample surface which had been indicated by the very weak -OH bending vibration. The FTIR spectral pattern of either S450 or S650 showed bands at 704, 860 and 1070 cm<sup>-1</sup>, indicating both samples were identical, which are due to the presence of Sr-O bonds in both the samples [18]. However, the intensity of

the peaks reduced compared to that of the pure oxide samples implying the decrease of Sr-O bond strength. Nevertheless, characteristics peaks of the Zr-O bonds are observed in all the four FTIR spectra. An observable change was found in the FTIR spectra of S850 and S1050 samples where a new band at 545 cm<sup>-1</sup> originated disappearing weak bands. This new band is probably due to the formation of Sr-O-Zr bond in S850 and S1050. Thus, it can be concluded that phase pure SrZrO<sub>3</sub> samples can be obtained by incinerating mixed hydrous Sr and Zr oxides at and above 850°C. No bands for either SrO or ZrO<sub>2</sub> are found in SrZrO<sub>3</sub> samples, which had also been indicated by the XRD studies.

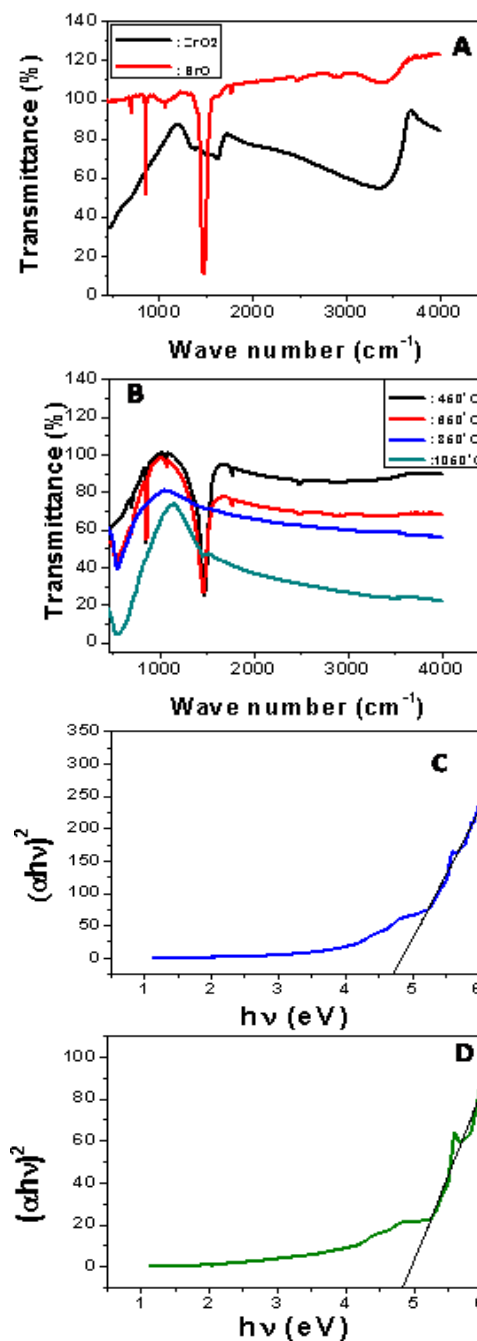
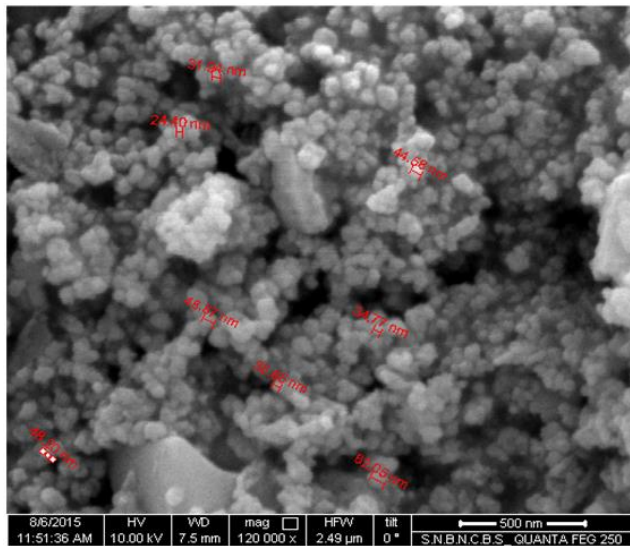


Fig. 2. FTIR spectra of (A) pure oxides and (B) S450, S650, S850 and S1050 samples, including the plots of  $(\alpha hv)^2$  versus  $h\nu$  for (A) S-850 and (B) S-1050 for band gaps.

In C and D of **Fig. 2** shows the Tauc plots [19]  $[(ah\nu)^2$  versus  $h\nu$ ] for band gap of SrZrO<sub>3</sub> (S850 and S1050) samples. The band gap (eV) that estimated for S850 and S1050 samples is 4.71 and 4.83, respectively, and the values are ranged in of the semiconducting materials and direct in nature. Despite the band gap values are close to each other, yet it increased with increasing incineration temperature. The increase of band gap with annealing temperature can be ascribed to the removal of impurities and defects that created intermediary energy levels in the band gap region of SrZrO<sub>3</sub> powder [20].

**Fig. 3** shows the FESEM image of the as-prepared S850 sample of SrZrO<sub>3</sub> only for surface morphology and size of material particles. It shows clearly the presence of nanoballs (~ 40 nm) in agglomerated form with irregular surface. The dimensions of the nanoballs are found to be very close to that obtained from the XRD data employing.



**Fig. 3.** Field emission scanning electron microscopic (FESEM) image of S850 sample.

Dielectric and ac conductivity relaxation processes in SrZrO<sub>3</sub> (S850) nanocrystals were investigated in detail. The plots in A of **Fig. 4** indicated the dispersion in  $\epsilon'$  at low frequency regions ( $< 1$  kHz) for the S850 sample of SrZrO<sub>3</sub> at six different temperatures, attributing the grain boundary contribution due to trapping of mobile charge carriers which provided high value of the dielectric constant. The plots in B of **Fig. 4** ( $Z''$  versus  $f$ ) described the impedance spectra as investigated at six different temperatures of SrZrO<sub>3</sub> (S850) sample. The  $Z''$  versus  $f$  plots (B in **Fig. 4**) clearly depicted only one electrical response due to grains in each case (marked by arrow in the figure). The response frequency ( $f_{\text{grain}}$ ) is found to be temperature dependent and varies from 1740 Hz to 5627 Hz as the temperature of the SrZrO<sub>3</sub> pellet changes from 24°C to 180°C. No peaks related to grain boundary response (low frequency) had been observed in our study. The grain boundary response is expected to be appeared at very low frequency regions ( $< 10$  Hz), which are limited to our frequency regions of investigations. The relaxation time due to grains has been estimated from the relaxation frequencies ( $\tau_{\text{grain}} = 1/2\pi f_{\text{grain}}$ ) are varies with temperature (92  $\mu\text{s}$  - 28  $\mu\text{s}$ ).

The plots in C of **Fig. 4** depicted the variation of dielectric loss,  $\tan(\delta)$  with frequency for the temperatures, which was investigated for the S850 sample of SrZrO<sub>3</sub>. Low dielectric losses and high values of dielectric constant indicated the suitability of SrZrO<sub>3</sub> for the wide range of applications in various devices.

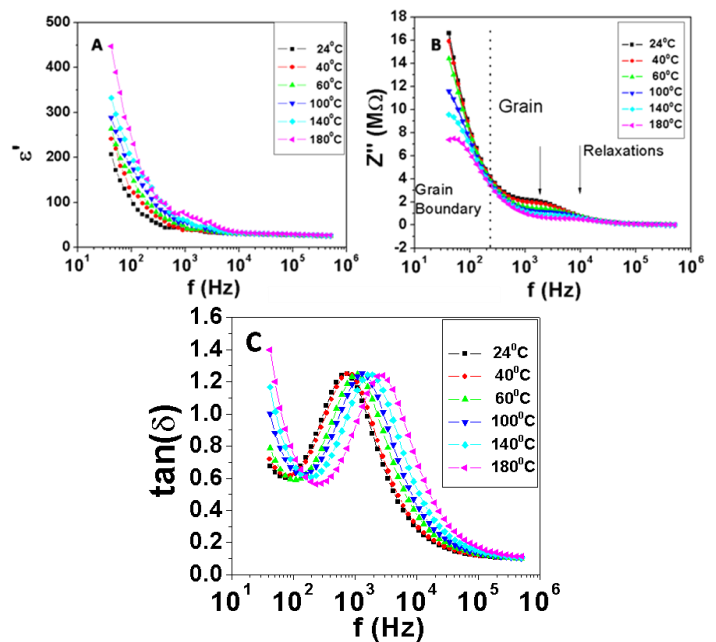


**Fig. 4.** The plots of (A) dielectric constant vs. frequency, (B) impedance vs. frequency and (C) dielectric loss spectra of S-850 sample of SrZrO<sub>3</sub>.

The plots in A of **Fig. 5** depicted the variation of ac-conductivity with frequency of S850 sample of SrZrO<sub>3</sub> at investigated six different temperatures. It is revealed that the ac-conductivity of the sample shows a weak dependence on the temperature, and remained flat at low frequency regions (42 Hz to 10 kHz).

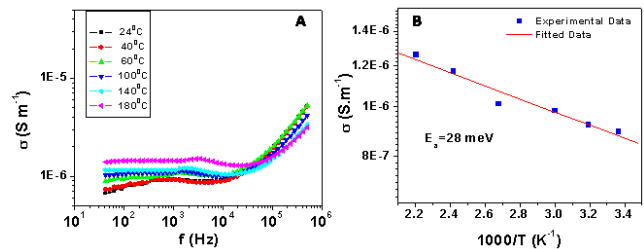


**Fig. 5.** The plots of (A) ac-conductivity vs. frequency (B) conductivity vs. temperature of S-850 sample of SrZrO<sub>3</sub>.

As the frequency increased ( $> 10$  kHz), the curves became dispersive and obeyed the universal power law  $\sigma' = \sigma_{\text{dc}} + \text{constant} \times f^m$ ,  $0 < m < 1$ ). Using the ac-conductivity data, the thermal activation energy ( $E_a$ ) had been calculated to be 28 meV at 10 kHz from the slope of the fitted line (B of **Fig. 5**) using the well known Arrhenius relation.

$$\sigma_{ac} = \sigma_0 \exp(-E_a/k_B T)$$

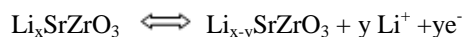
where,  $\sigma_0$  is a constant,  $k_B$  is the Boltzmann constant and  $T$  is the absolute temperature. Data presented in A of **Fig. 5**

suggested that in the frequency range 42 Hz to 10 kHz the conductivity is independent of frequency in all the temperatures, which may be attributed to the contribution of free charges available in the sample. In the frequency ranges from 10 kHz and above, the conductivity rises steadily and shows dispersions. Considering the above frequency dependent behavior of ac-conductivity together with low thermal activation energy (28 meV), it can be concluded that hopping conduction of mobile charge carriers is responsible for the electrical conduction in grains of the SrZrO<sub>3</sub> nanomaterial sample, which is found to be similar in behavior with some other disordered materials [21, 22].

The electrochemical characteristics of the S850 and S1050 samples of SrZrO<sub>3</sub> were studied using cyclic voltammetry (A and B of Fig. 6) in acetonitrile solvent containing 1M LiClO<sub>4</sub> as the electrolyte over the potential window (-0.6 V to +0.6 V). The shapes of the curves suggested that the capacity of the SrZrO<sub>3</sub> samples results from pseudo-capacitive capacitance. It can be assumed that the Faradaic pseudo-capacitive property is not the outcome of any redox reaction on the SrZrO<sub>3</sub> surface, since there is no possibility of set up of any redox reaction under such condition. Thus the pseudo-capacitive charging of the material is due to the diffusion of Li<sup>+</sup> ions into the perovskite structure of SrZrO<sub>3</sub>. This lithiation process into the perovskite structure of SrZrO<sub>3</sub> could be represented by the equation:



The delithiation process could be represented by the following equation:



The specific capacitance ( $C_s$ ) of the samples were estimated from the cyclic voltammetric (CV) measurement using the following relation,

$$C_s = \frac{\int_{V_1}^{V_2} I(v) dv}{(V_2 - V_1) \nu m}$$

where,  $I(V)$  is the instantaneous current in CV,  $\nu$  is the scan rate,  $m$  is the mass of the electroactive material and  $(V_2 - V_1)$  is the potential window. The specific capacitances 11.8 F/g and 24.2 F/g for the samples S850 and S1050, respectively, were found to be for the scan rate 20 mV/s. The Galvanostatic charge-discharge curve is shown in B of Fig. 6 at a current density 1mA/cm<sup>2</sup>. The specific capacitances ( $C_s$ ) of the samples were also measured from the linear slope of the discharging curve using the following formula:

$$C_s = \frac{I \Delta t}{m \Delta V}$$

where,  $I$  is the discharge current,  $\Delta t$  is the discharge time,  $\Delta V$  is the potential drop in the discharge progress and  $m$  is the active mass of the electrode. The specific capacitances are 11.0 and 23.0 F/g for the samples S850 and S1050,

respectively, are very close to the values obtained by CV measurements.

The electrochemical impedance spectra of both the samples are shown in C of Fig. 6 (Nyquist plot) within the frequency range 100 kHz-10 MHz at room temperature. The shape of the curves is very much helpful to elucidate the electron or ion transfer kinetics and diffusion characteristics. In the lower frequency region, the imaginary part of the impedance ( $Z''$ ) sharply increased ( $\sim 63^\circ$  straight line) demonstrating the capacitive behavior of the samples, which is the behavior that observed for the porous materials [23]. This is the first report for the electrochemical behaviors of SrZrO<sub>3</sub> porous powder. Further, investigation is required to enhance specific capacitance of SrZrO<sub>3</sub> electrode for using SrZrO<sub>3</sub> as a cathode material in electrochemical cells.

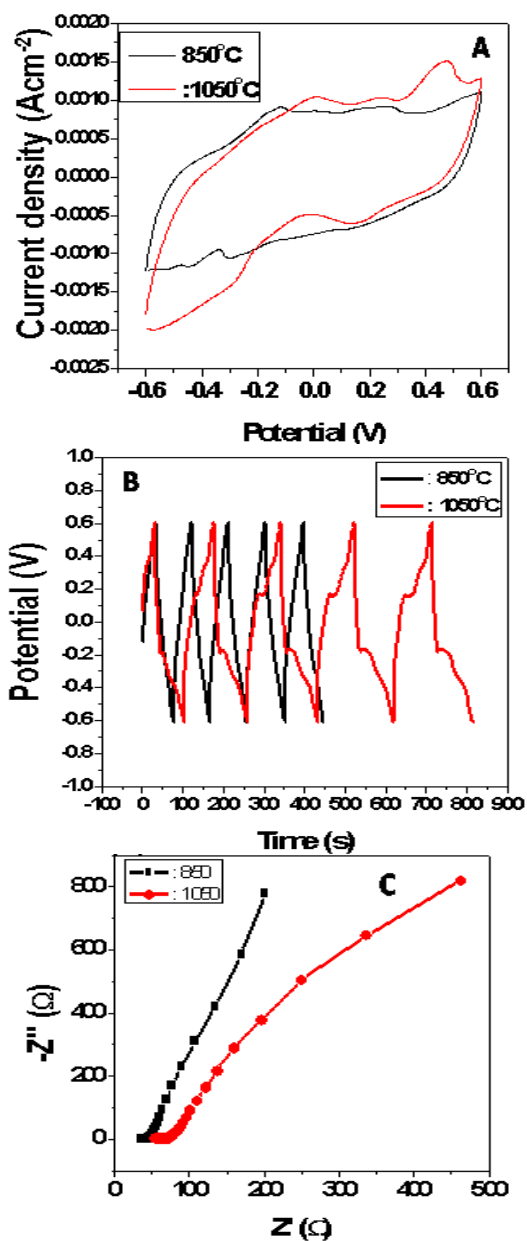


Fig. 6. The cyclic voltammograms (A) current density versus potential, (B) potential vs. time and (C) Nyquist plot within the frequency range 100 kHz to 10 MHz of S850 and S1050 samples of SrZrO<sub>3</sub> at room temperature.

## Conclusion

Strontium-zirconate ( $\text{SrZrO}_3$ ) samples prepared by hydroxide gel formation-annealing method were cost-effective and green materials, which were crystalline and nanostructured with band gap value in semiconducting range. The materials composed of Sr-O-Zr bonded phase as confirmed from the FTIR spectra. Surface morphology of  $\text{SrZrO}_3$  (S850) sample was irregular with agglomerized nano balls. Temperature dependent ac-conductivity analyses of S850 sample showed semiconducting behavior of the material. The S850 sample of  $\text{SrZrO}_3$  inclined to a dielectric material from the high dielectric constant and low dielectric loss. The  $\text{SrZrO}_3$  (S850 and S1050) material showed the behavior of pseudo-capacitive capacitance, which had been confirmed from the analyses of Cyclic Voltammograms. The temperature and frequency dependent behavior of ac-conductivity together with low thermal activation energy (28 meV) attributed the hopping conduction of mobile charge carriers in the grains of the  $\text{SrZrO}_3$  nanomaterial. Thus it can be concluded that, as-prepared nanocrystals of  $\text{SrZrO}_3$  have high dielectric constant ( $\epsilon'$ ) and the material can be used as a dielectric and pseudo capacitive material.

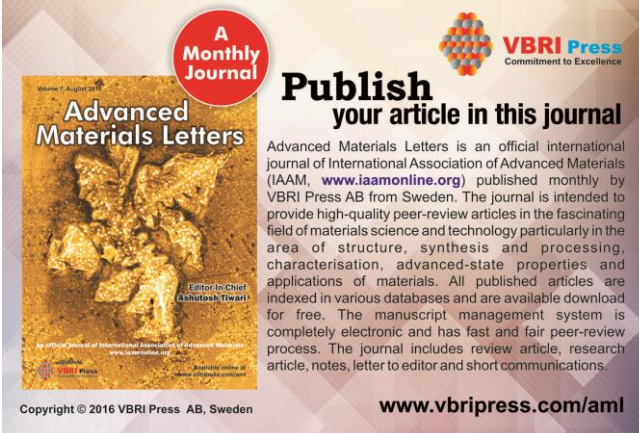
## Acknowledgements

Authors are thankful to the Head, Department of Applied Chemistry (Post Graduate) and the Principal Maharaj, Ramakrishna Mission Vidyamandira, Belur Math, Howrah, West Bengal (India) for laboratory facilities to carry out this work.

## Reference

- Osaka, T.; Numako, C.; Koto, K.; *Mater. Res. Bull.* **1999**, *34*, 11.  
DOI: <http://dx.doi.org/10.1088/0953-8984/13/11/304>
- Longo, V.; Richiasdiello, F.; Shaizero, O.; in: R. Carlsson, S. Carlsson (Eds.), *Science of Ceramics II, Swedish Ceramic Society*, **1981**, p-467.
- Longo, V.M.; Cavalcante, L.S.; de Figueiredo, A.T.; Santos, L.P.S.; Longo, E.; Varela, J.A.; Sambrano, J.R.; Paskocimas, C. A.; De Vicente, F.S.; Hernandez, A.C.; *Appl. Phys. Lett.* **2007**, *90*, 091906.  
DOI: <http://dx.doi.org/10.1063/1.2709992>
- Nair, J.; Nair, P.; Doesburg, E. B. M.; Van Ommen, J. G.; Ross, J. R. H.; Burggraaf, A. J.; Mizukami, F.; *J. Mater. Sci.* **1998**, *33*, 4517.
- Shende, R.V.; Krueger, D.S.; Jr. Rossetti, G. A.; Lombardo, S.J.; *J. Am. Ceram. Soc.* **2001**, *84*, 1648.  
DOI: [10.1111/j.1151-2916.2001.tb00893.x](http://dx.doi.org/10.1111/j.1151-2916.2001.tb00893.x)
- Bhavsar, R. S.; Limsay, R. H.; Talwatkar, C. B.; *Ind. J. Chem. Technol.* **2012**, *19*, 124.
- Liu, C. -Y.; Tseng, T. -Y. *J. Phys. D: Appl. Phys.* **2007**, *40*, 2157.  
DOI: <http://dx.doi.org/10.1088/0022-3727/40/7/045>
- Potdar, H. S.; Deshpande, S. B.; Patil, A. J.; Deshpande, A. S.; Kholam, Y. B.; Date, S. K.; *Mater. Chem. Phys.* **2000**, *65*, 178.  
DOI: [10.1016/S0254-0584\(00\)00238-8](http://dx.doi.org/10.1016/S0254-0584(00)00238-8)
- Lencka, M. M.; Nielsen, E.; Anderko, A.; Riman, R. E.; *Chem. Mater.* **1997**, *9*, 1116.  
DOI: [10.1021/cm960444n](http://dx.doi.org/10.1021/cm960444n)
- Homes, C. C.; Vogt, T.; Shapiro, S. M.; Wakimoto, S.; Ramirez, A. P.; *Science* **2001**, *293*, 673.  
DOI: [10.1126/science.1061655](http://dx.doi.org/10.1126/science.1061655)
- Li, W.; Schwartz, R.W.; *Appl. Phys. Lett.* **2006**, *89*, 242906.  
DOI: <http://dx.doi.org/10.1063/1.2405382>
- Malghe, Y. S.; Yadav, U. C.; *J. Therm. Anal. Calorim.* **2015**, *122*, 589.  
DOI: [10.1007/s10973-015-4804-9](http://dx.doi.org/10.1007/s10973-015-4804-9)
- Al-Hartomy, O. A.; Ubaidullah, M.; Kumar, D.; Madani, J. H.; Ahmad, T.; *J. Mater. Res.* **2013**, *28*, 1070.  
DOI: <http://dx.doi.org/10.1557/jmr.2013.40>

- Al-Hartomy, O. A.; Ubaidullah, M.; Ahmad, T.; *J. Mater. Res.* **2013**, *40*, 1.  
DOI: <http://dx.doi.org/10.1557/jmr.2013.40>
- Sen, P.; Dey, A.; *Electrochim. Acta.* **2010**, *55*, 4677.  
DOI: [10.1016/j.electacta.2010.03.077](http://dx.doi.org/10.1016/j.electacta.2010.03.077)
- Motsuda, T.; Yamanaka, S.; Kurosaki, K.; Kobayashi, S. I.; *J. Alloys Compd.* **2003**, *351*, 43.  
DOI: [10.1016/S0925-8388\(02\)01068-X](http://dx.doi.org/10.1016/S0925-8388(02)01068-X)
- Rudel, R.; Ferenczy, F. Z.; *J. Physiol.* **1979**, *290*, 317.  
DOI: [10.1113/jphysiol.1979.sp012773/pdf](http://dx.doi.org/10.1113/jphysiol.1979.sp012773/pdf)
- de O. Lima, J. R.; Ghani, Y. A.; da Silva, R. B.; Batista, F. M. C.; Bini, R. A.; Varanda, L. C.; de Oliveira, J. E.; *Applied Catalysis A: General.* **2012**, *445-446*, 76.  
DOI: [10.1016/j.apcata.2012.08.005](http://dx.doi.org/10.1016/j.apcata.2012.08.005)
- Tumuluri, A.; Naidu, K. L. Naidu; Raju, K. C. J.; *Inter. J. Chem. Tech. Res.* **2014**, *6*, 3353.
- Cavalcante, L. S.; Simoes, A. Z.; Sczancoski, J. C.; Longo, V. M.; Erlo, R.; Escote, M. T.; Longo, E.; *Solid State Sciences* **2007**, *9*, 1020.  
DOI: [10.1016/j.solidstatesciences.2007.07.019](http://dx.doi.org/10.1016/j.solidstatesciences.2007.07.019)
- Elliott, S. R.; *Adv. Phys.* **1987**, *36*, 135.  
DOI: [10.1080/00018738700101971](http://dx.doi.org/10.1080/00018738700101971)
- El-Mallah, H. M.; AC Electrical Conductivity and Dielectric Properties of Perovskite (Pb, Ca)TiO<sub>3</sub> Ceramic. *Acta Physica Polonica A.* **2012**, *122*, 174.
- Yagmur, V.; Atalay, F. E.; Kaya, H.; Avcu, D.; Aydogmus, E.; Electrochemical Capacitance of Cobalt Oxide Nanotubes on Nickel Foam. *Acta Physica Polonica A.* **2013**, *123*, 215.  
DOI: [12693/APhysPolA.123.215](http://dx.doi.org/10.12693/APhysPolA.123.215)



**A Monthly Journal**

**Publish your article in this journal**

Advanced Materials Letters is an official international journal of International Association of Advanced Materials (IAAM, [www.iaamonline.org](http://www.iaamonline.org)) published monthly by VBRI Press AB from Sweden. The journal is intended to provide high-quality peer-review articles in the fascinating field of materials science and technology particularly in the area of structure, synthesis and processing, characterisation, advanced-state properties and applications of materials. All published articles are indexed in various databases and are available download for free. The manuscript management system is completely electronic and has fast and fair peer-review process. The journal includes review article, research article, notes, letter to editor and short communications.

[www.vbripress.com/aml](http://www.vbripress.com/aml)

Copyright © 2016 VBRI Press AB, Sweden